Electronic Supplementary Material (ESI) for Physical Chemistry Chemical Physics.
This journal is © the Owner Societies 2017

Supporting information

for

Insights into water-mediated ion clustering in aqueous $CaSO_4$ solutions: Pre-nucleation clusters characteristics studied by DFT and molecular dynamics

Hui-Ji Li[a], Dan Yan[a], Hou-Qin Cai[a], Hai-Bo Yi[a*], Xiao-Bo Min[b*], Fei-Fei Xia[c*]

[a]State Key Laboratory of Chemo/Biosensing and Chemometrics, College of Chemistry and Chemical Engineering, Hunan University, Changsha 410082, People's Republic of China

[b]Chinese National Engineering Research Center for Control & Treatment of Heavy Metal Pollution, School of Metallurgy and Environment, Central South University, Changsha 410083, China

[c]Institute of Functional Nano & Soft Materials (FUNSOM), Collaborative Innovation Center of Suzhou Nano Science and Technology (NANO-CIC), Jiangsu Key Laboratory for Carbon-Based Functional Materials & Devices, Soochow University, Suzhou 215123, Jiangsu, P. R. China

Email: hbyi@hnu.edu.cn (H.-B. Yi); mxbcsu@163.com (X.-B. Min); xff7461198@163.com (F.-F. Xia).

Table S1 Force-Field Parameters for Ions and Water in Molecular Dynamics Simulations.[1-3]

Atom	ε (kcal/mol)	σ (Å)	q (e)
Ca^{2+}	0.450	2.361	2.000
S (sulfur in SO_4^{2-})	0.250	3.550	2.000
OS (oxygen in SO_4^{2-})	0.200	3.150	−1.000
O (oxygen in H_2O)	0.155	3.166	−0.848
H (hydrogen in H_2O)	0.000	0.000	0.424

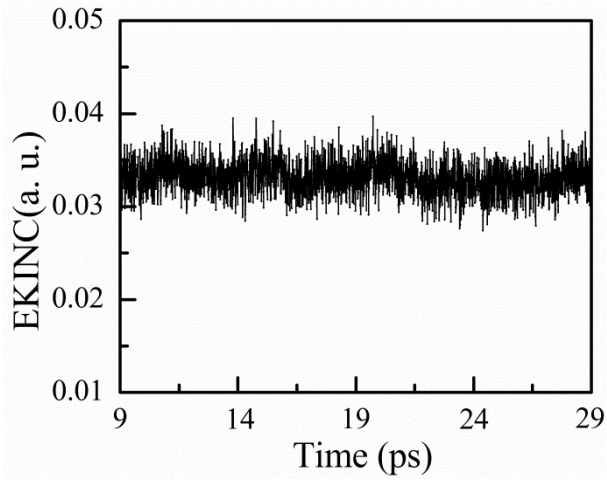

Fig. S1 The classical kinetic energy for the electronic degrees of freedom vs the CPMD simulation time during last 20.0 ps run.

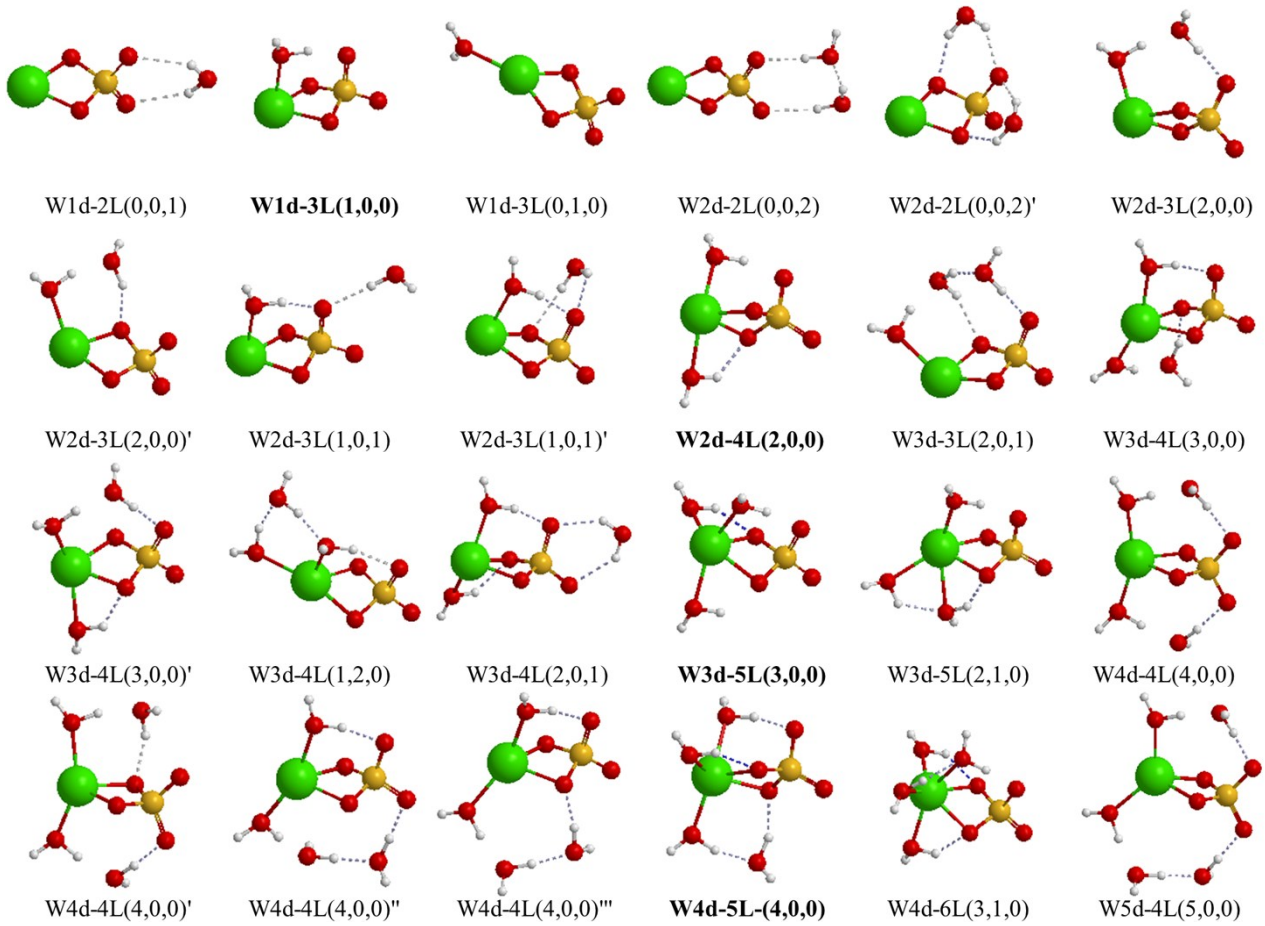

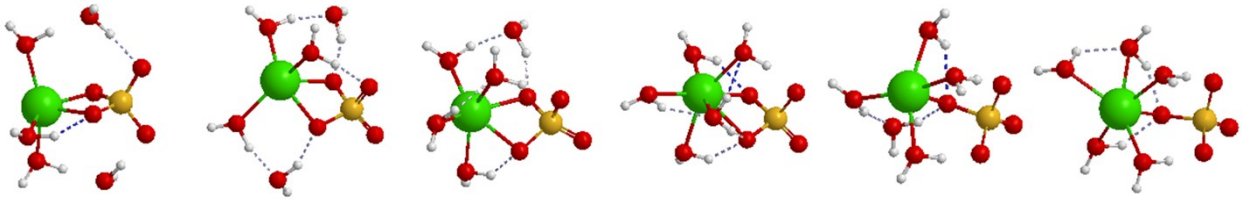

W5d-5L(5,0,0) **W5d-5L(5,0,0)'** **W5d-6L(4,1,0)** W5d-7L(4,1,0) W5m-5L(5,0,0) W5m-6L(4,1,0)

Fig. S2 Typical structures of $[CaSO_4(H_2O)_n]$ (n = 1–5) clusters obtained at the B3LYP/aVDZ level. Gray dotted lines indicate hydrogen bonds.

Table S2 Structural and energy parameters for $[CaSO_4(H_2O)_n]$ (n = 1–5) clusters at the B3LYP/aVDZ level in the gas phase.

geometries	structural parameters[a]			energy parameters[b]	
	$R_{Ca\text{-}S}$	$R_{Ca\text{-}OS}$	$R_{Ca\text{-}O}$	ΔE_0	ΔG
W1d-2L(0,0,1)	2.74	2.07	-	-516.0	-500.9
W1d-3L(1,0,0)	**2.72**	**2.15**	**2.28**	**-540.6**	**-522.8**
W1d-3L(0,1,0)	2.76	2.10	2.28	-523.2	-505.8
W2d-2L(0,0,2)	2.74	2.08	-	-521.2	-497.5
W2d-2L(0,0,2)'	2.77	2.08	-	-514.0	-487.3
W2d-3L(2,0,0)	2.78	2.13	2.28	-555.9	-529.0
W2d-3L(2,0,0)'	2.81	2.13	2.32	-550.0	-523.9
W2d-3L(1,0,1)	2.73	2.15	2.27	-545.3	-520.4
W2d-3L(1,0,1)'	2.74	2.15	2.29	-543.6	-516.0
W2d-4L(2,0,0)	**2.78**	**2.20**	**2.33**	-561.8	**-534.9**
W3d-3L(2,0,1)	2.81	2.15	2.27	-564.6	-528.9
W3d-4L(3,0,0)	2.79	2.21	2.32	-578.3	-542.1
W3d-4L(3,0,0)'	2.83	2.19	2.33	-576.9	-540.9
W3d-4L(1,2,0)	2.73	2.16	2.25	-557.6	-519.6
W3d-4L(2,0,1)	2.78	2.20	2.33	-564.1	-527.4
W3d-5L(3,0,0)	**2.83**	**2.25**	**2.36**	**-580.2**	**-544.5**
W3d-5L(2,1,0)	2.81	2.23	2.43	-577.7	-541.6
W4d-4L(4,0,0)	2.81	2.19	2.32	-595.3	-549.5
W4d-4L(4,0,0)'	2.84	2.20	2.31	-593.4	-547.8
W4d-4L(4,0,0)"	2.77	2.20	2.33	-589.1	-544.1
W4d-4L(4,0,0)"'	2.79	2.21	2.32	-588.9	-544.0
W4d-5L-(4,0,0)	**2.85**	**2.26**	**2.36**	**-595.4**	**-550.2**
W4d-6L(3,1,0)	2.88	2.29	2.42	-595.2	-550.0
W5d-4L(5,0,0)	2.82	2.20	2.31	-605.2	-551.3
W5d-5L(5,0,0)	**2.87**	**2.24**	**2.37**	**-610.2**	**-555.2**
W5d-5L(5,0,0)'	**2.88**	**2.28**	**2.35**	**-609.7**	**-555.3**
W5d-6L(4,1,0)	**2.91**	**2.31**	**2.42**	**-609.8**	**-555.0**
W5d-7L(4,1,0)	2.93	2.35	2.47	-607.3	-553.2
W5m-5L(5,0,0)	3.20	2.23	2.36	-603.3	-548.8
W5m-6L(4,1,0)	3.26	2.27	2.42	-602.1	-547.4

[a] $R_{Ca\text{-}S}$, $R_{Ca\text{-}OS}$, and $R_{Ca\text{-}O}$ are the Ca-S, averaged Ca-OS (oxygen of SO_4^{2-}) and Ca-O (oxygen of H_2O) distances in angstrom for $[CaSO_4(H_2O)_n]$ (n = 1–5) clusters. [b] ΔE_0 is the zero-point corrected binding energy, and ΔG is the free energy in the gas phase at 298 K and 1 atm. All the energies are in kcal/mol.

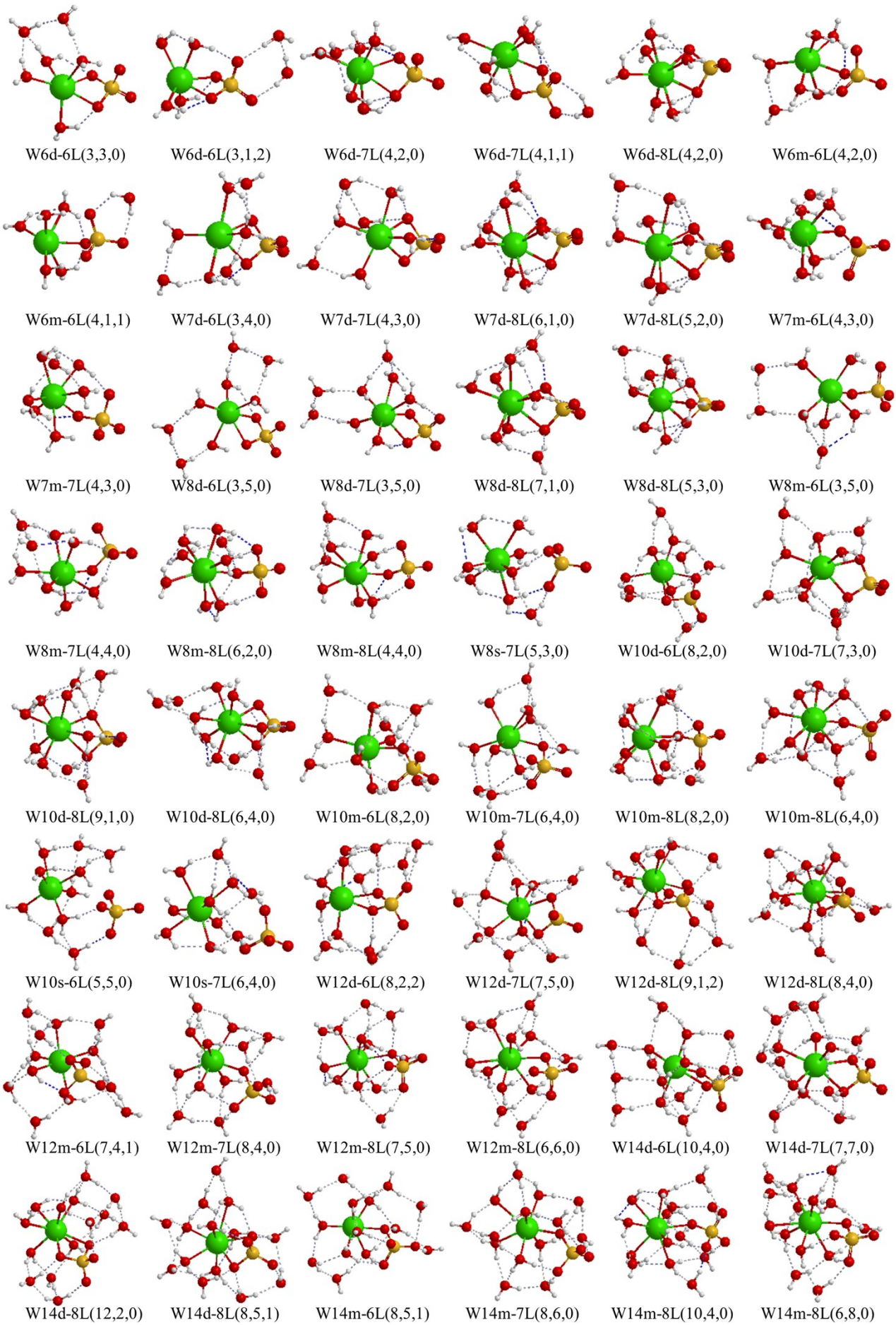

Fig. S3 Additional typical structures of $[CaSO_4(H_2O)_n]$ (n = 6–8, 10, 12, 14) clusters obtained at the

B3LYP/aVDZ level. Gray dotted lines indicate hydrogen bonds. It can be found that these conformers with more water molecules in site-B and site-C of Scheme 1 are less stable than their isomers with more water molecules in site-A, as shown in Fig. 1.

Table S3 Additional typical structural and energy parameters for [$CaSO_4(H_2O)_n$] (n = 6–8, 10, 12, 14) clusters at the B3LYP/aVDZ level in the gas and aqueous phases.

geometries	structural parameter[a]			energy parameters[b]			
				gas phase		aqueous phase	
	$R_{Ca\text{-}S}$	$R_{Ca\text{-}OS}$	$R_{Ca\text{-}O}$	ΔE_0	ΔG	$\Delta E_{0,\,solv}$	ΔG_{solv}
W6d-6L(3,3,0)	2.89	2.31	2.42	-614.9	-550.2	-653.7	-589.0
W6d-6L(3,1,2)	2.88	2.29	2.42	-605.6	-544.1	-651.3	-589.9
W6d-7L(4,2,0)	2.95	2.37	2.46	-617.7	-552.4	-651.6	-586.2
W6d-7L(4,1,1)	2.94	2.36	2.46	-603.2	-538.9	-641.6	-577.3
W6d-8L(4,2,0)	2.99	2.39	2.52	-616.1	-554.3	-648.2	-586.4
W6m-6L(4,2,0)	3.36	2.30	2.42	-612.7	-548.7	-653.5	-589.6
W6m-6L(4,1,1)	3.28	2.27	2.41	-596.4	-530.3	-641.1	-575.1
W7d-6L(3,4,0)	2.88	2.29	2.47	-618.9	-544.6	-658.5	-584.2
W7d-7L(4,3,0)	2.94	2.38	2.48	-622.2	-548.3	-656.5	-582.6
W7d-8L(6,1,0)	3.03	2.41	2.52	-629.2	-553.9	-655.8	-580.5
W7d-8L(5,2,0)	3.01	2.40	2.53	-626.3	-552.2	-655.2	-581.1
W7m-6L(4,3,0)	3.16	2.30	2.42	-625.6	-551.4	-658.9	-584.7
W7m-7L(4,3,0)	3.24	2.31	2.49	-625.4	-550.2	-656.3	-581.0
W8d-6L(3,5,0)	2.92	2.33	2.43	-629.9	-548.5	-666.5	-585.1
W8d-7L(3,5,0)	2.91	2.31	2.50	-626.3	-543.8	-663.1	-580.6
W8d-8L(7,1,0)	3.05	2.42	2.52	-641.9	-557.4	-665.2	-580.7
W8d-8L(5,3,0)	3.02	2.41	2.54	-632.0	-547.8	-659.4	-575.1
W8m-6L(3,5,0)	3.35	2.23	2.45	-623.3	-540.9	-665.6	-583.1
W8m-7L(4,4,0)	3.25	2.30	2.47	-632.0	-546.9	-663.2	-578.0
W8m-8L(6,2,0)	3.34	2.35	2.54	-636.1	-551.5	-662.7	-578.1
W8m-8L(4,4,0)	3.32	2.33	2.55	-633.7	-548.6	-662.3	-577.3
W8s-7L(5,3,0)	3.81	3.55	2.46	-627.7	-543.3	-660.2	-575.8
W10d-6L(8,2,0)	2.97	2.33	2.41	-664.9	-561.5	-686.6	-583.2
W10d-7L(7,3,0)	3.06	2.37	2.48	-655.8	-553.5	-680.3	-578.0
W10d-8L(9,1,0)	3.07	2.43	2.54	-662.1	-559.1	-679.3	-576.4
W10d-8L(6,4,0)	2.98	2.35	2.56	-654.6	-551.1	-676.7	-573.2
W10m-6L(7,3,0)	3.44	2.28	2.44	-661.7	-556.7	-684.8	-579.7
W10m-7L(6,4,0)	3.47	2.44	2.47	-659.0	-553.6	-681.3	-576.0
W10m-8L(8,2,0)	3.44	2.40	2.51	-655.4	-550.4	-674.9	-570.0
W10m-8L(6,4,0)	3.55	2.37	2.53	-657.2	-552.6	-631.0	-526.4
W10s-6L(5,5,0)	4.36	-	2.39	-654.3	-549.1	-684.4	-579.3
W10s-7L(6,4,0)	4.31	-	2.46	-646.9	-542.3	-677.0	-572.4
W12d-6L(8,2,2)	3.04	2.39	2.38	-684.5	-562.9	-702.8	-581.2
W12d-7L(7,5,0)	3.07	2.38	2.49	-670.4	-548.7	-692.1	-570.4
W12d-8L(9,1,2)	3.08	2.45	2.53	-678.0	-556.4	-689.9	-568.2
W12d-8L(8,4,0)	3.06	2.43	2.55	-673.8	-550.1	-689.1	-565.4
W12m-6L(7,4,1)	3.48	2.38	2.42	-676.7	-552.8	-697.0	-573.2
W12m-7L(8,4,0)	3.59	2.29	2.49	-678.1	-553.6	-696.1	-571.6
W12m-8L(7,5,0)	3.48	2.44	2.54	-674.1	-549.4	-689.1	-564.4
W12m-8L(6,6,0)	3.45	2.42	2.55	-670.3	-546.1	-687.7	-563.5
W14d-6L(10,4,0)	3.04	2.36	2.42	-693.1	-551.6	-712.8	-571.3

W14d-7L(7,7,0)	3.02	2.40	2.51	-689.8	-546.9	-705.6	-562.7
W14d-8L(12,2,0)	3.12	2.45	2.52	-702.3	-557.9	-709.7	-565.3
W14d-8L(8,5,1)	3.04	2.42	2.56	-692.5	-549.1	-703.0	-559.5
W14m-6L(8,5,1)	3.48	2.31	2.42	-619.9	-550.0	-709.0	-567.1
W14m-7L(8,6,0)	3.57	2.29	2.52	-693.8	-549.0	-710.5	-565.7
W14m-8L(10,4,0)	3.64	2.33	2.54	-695.1	-551.8	-706.3	-563.0
W14m-8L(6,8,0)	3.42	2.41	2.54	-682.9	-539.3	-698.5	-554.9

[a]$R_{Ca\text{-}S}$, $R_{Ca\text{-}OS}$, and $R_{Ca\text{-}O}$ are the Ca-S, averaged Ca-OS (oxygen of SO_4^{2-}) and Ca-O (oxygen of H_2O) distances in angstrom of $[CaSO_4(H_2O)_n]$ (n = 6–8, 10, 12, 14) clusters. [b]ΔE_0 is the zero-point corrected binding energy, and ΔG is the free energy in the gas phase at 298 K and 1 atm. $\Delta E_{0,\ solv}$ and ΔG_{solv} in the aqueous phase were obtained at the PCM-B3LYP/aVDZ level. All the energies are in kcal/mol.

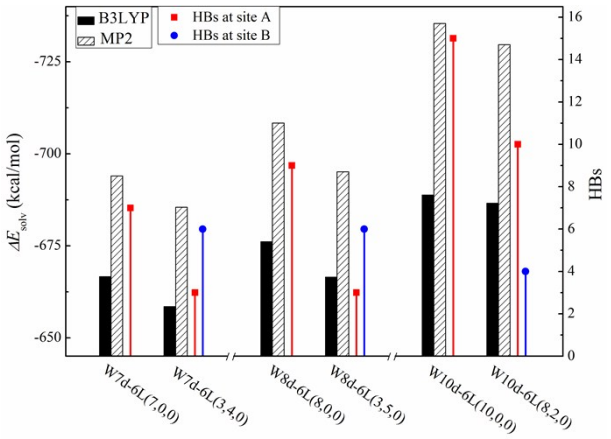

Fig. S4 Stabilization energy vs position of hydrogen bonds for typical $[CaSO_4(H_2O)_n]$ (n = 7, 8, 10) clusters at the B3LYP/aVDZ and MP2/aVDZ levels.

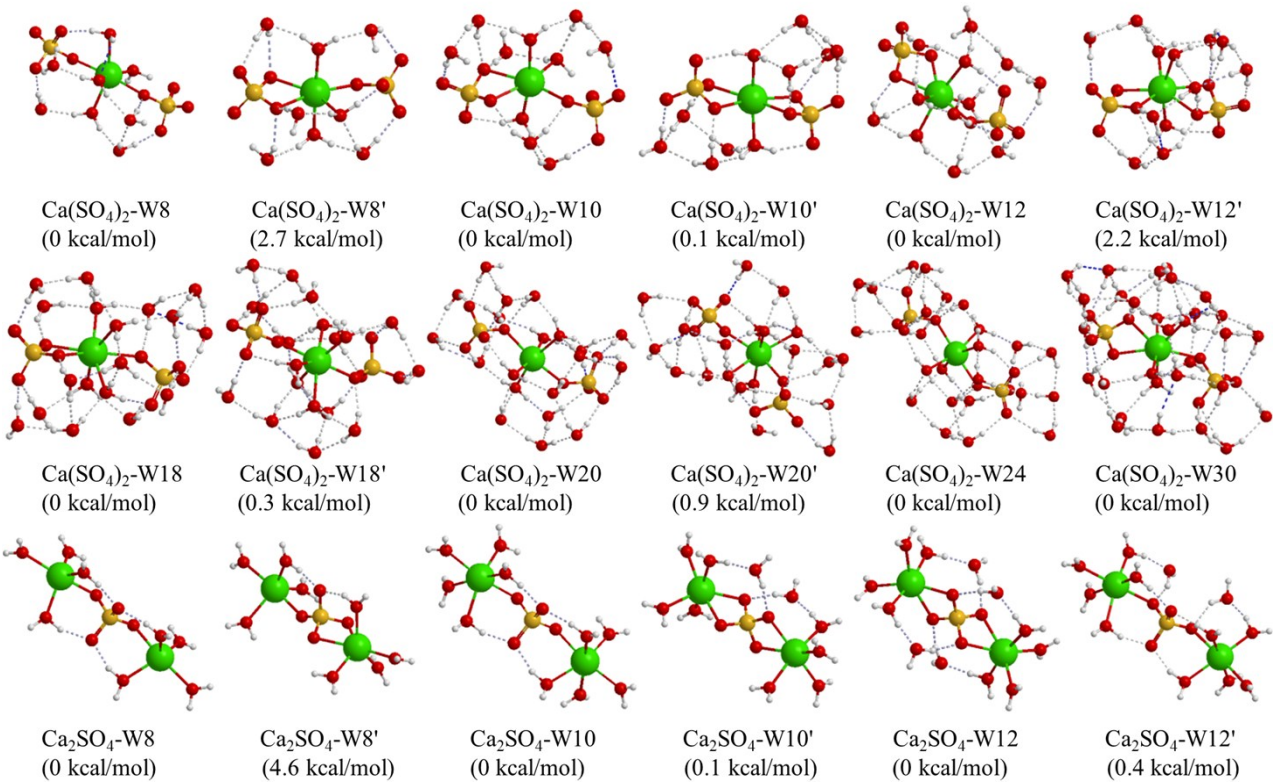

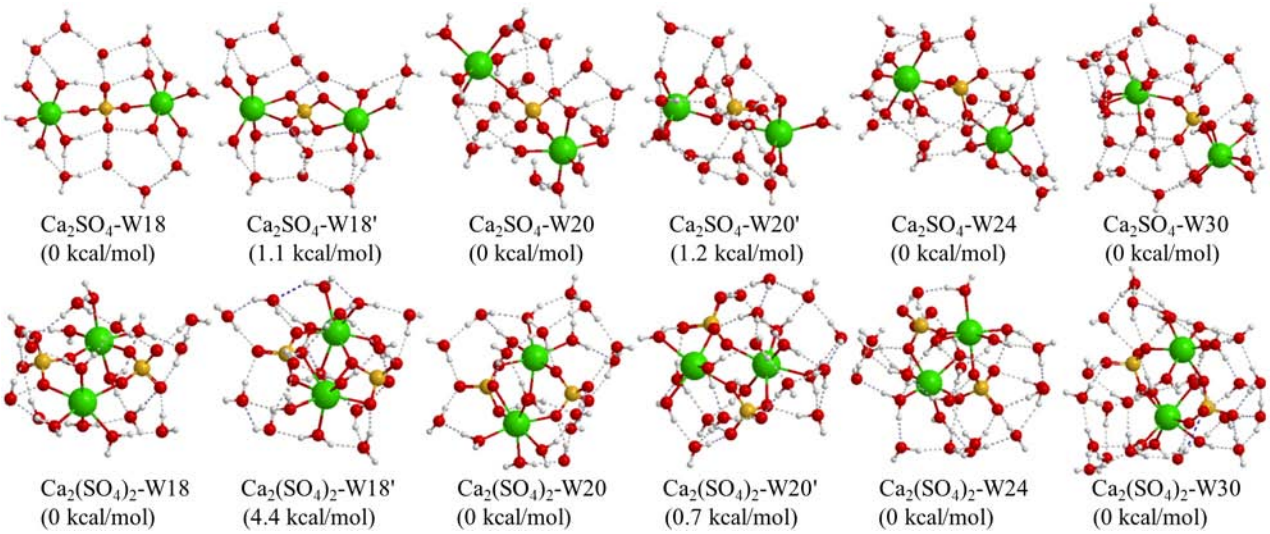

Fig. S5 Typical structures of $[Ca_x(SO_4)_y(H_2O)_n]^{2x-2y}$ (x, y= 1–2, n = 8, 10, 12, 18, 20, 24, 30) clusters obtained at the B3LYP/aVDZ level. Gray dotted lines indicate hydrogen bonds.

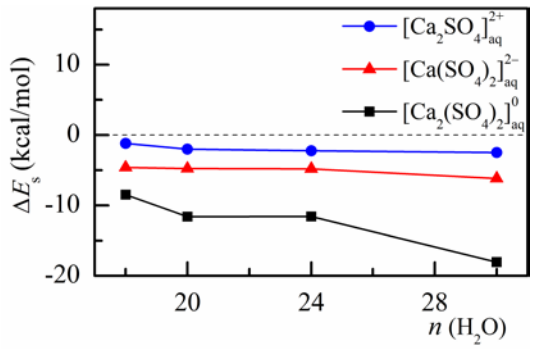

Fig. S6 Stabilization energies (ΔE_s) of $[Ca(SO_4)_2]^{2-}_{aq}$, $[Ca_2SO_4]^{2+}_{aq}$ and $[Ca_2(SO_4)_2]^{0}_{aq}$ species.

Meanwhile, the stabilities of various $[Ca_x(SO_4)_y]^{2x-2y}_{aq}$ (x, y = 1–2) species can be compared using the stabilization energies (ΔE_s):

$$\Delta E_s = E_{[Ca_x(SO_4)_y]^{2x-2y},aq} - E_{CaSO_4,aq} - (x-1)E_{Ca^{2+},aq} - (y-1)E_{SO_4^{2-},aq}$$

which correspond to the process

$$[CaSO_4]^0_{aq} + (x-1)Ca^{2+}_{aq} + (y-1)SO^{2-}_{4,aq} \rightleftharpoons [Ca_x(SO_4)_y]^{2x-2y}_{aq}$$

Since the solubility of $CaSO_4$ in an aqueous solution is quite low, the energies of Ca^{2+}_{aq}, $SO^{2-}_{4,aq}$, $[CaSO_4]^0_{aq}$ and $[Ca_x(SO_4)_y]^{2x-2y}_{aq}$ species can be estimated from their hydrated clusters, such as $[Ca(H_2O)_{18}]^{2+}$,[4] $[SO_4(H_2O)_{12}]^{2-}$, $[CaSO_4(H_2O)_{12}]$, and $[Ca_x(SO_4)_y(H_2O)_n]^{2x-2y}$ (n = 8, 10, 12, 14, 18, 20, 24, 30) clusters, at the PCM-B3LYP/aVDZ level ($E_{M,aq} = E_{[M(H_2O)_n],aq} - nE_{H_2O,l}$, M = Ca^{2+},

SO_4^{2-}, $[CaSO_4]^0$ and $[Ca_x(SO_4)_y]^{2x-2y}$). The energy of $H_2O(l)$ is estimated by the sum of the energy of gaseous water molecules and the evaporation energy (10.5 kcal/mol).[5]

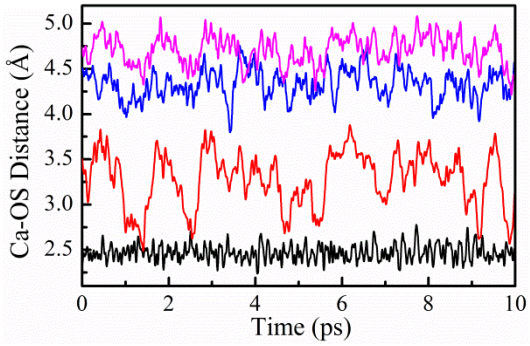

Fig. S7 Ca-OS (O site of the SO_4^{2-}) distance as a function of CPMD simulation time during a further 10 ps CPMD simulation with a time step of 5 a.u. and a fictitious mass of 600 a.u.

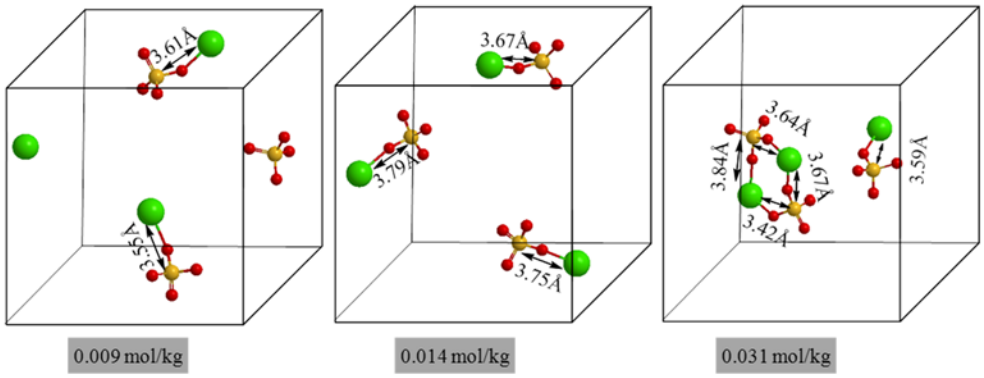

Fig. S8 Depictions of the systems with 0.009, 0.014, and 0.031 mol/kg concentrations after 10 ns MD simulations at 298 K. Water molecules have been removed to get a clear view of the ion-association situation between Ca^{2+} and SO_4^{2-} ions. The black arrow labels the Ca-S distance. These Ca-S distances in Fig. S8 slightly vibrate around the first peak of $g_{Ca-S}(r)$ (in Fig. 5(a)) at 3.67 Å.

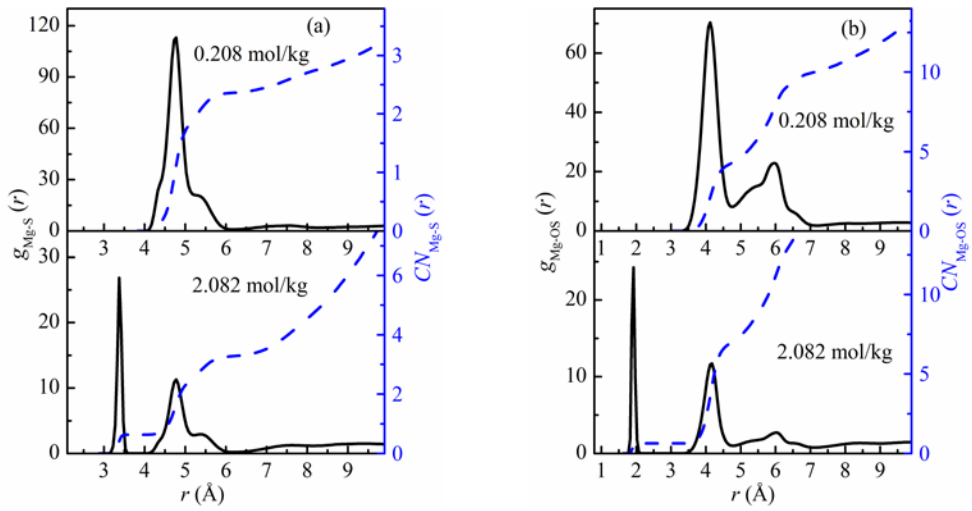

Fig. S9 The radial distribution function ($g(r)$) represented by the solid lines and the coordination number (CN)

represented by the dashed lines for Mg^{2+} and (a) the S site and (b) the O site (OS) of the SO_4^{2-} anion for different salt concentrations, as obtained from the last 4 ns of the classical MD run.

In the 0.208 mol/kg aqueous $MgSO_4$ solution, the first peak of $g_{Mg\text{-}S}(r)$ at 4.78 Å and $g_{Mg\text{-}OS}(r)$ at 4.13 Å in the Fig. S6 indicate that CIP conformers can not been found. However, the Mg-OS distance is at 1.93 Å, with the $CN_{Mg\text{-}OS}$ of 0.63, and the Mg-S distance is at 3.38 Å, with the $CN_{Mg\text{-}OS}$ of 0.63, in the 2.082 mol/kg aqueous $MgSO_4$ solution, which show that the CIP structures form at this concentration.

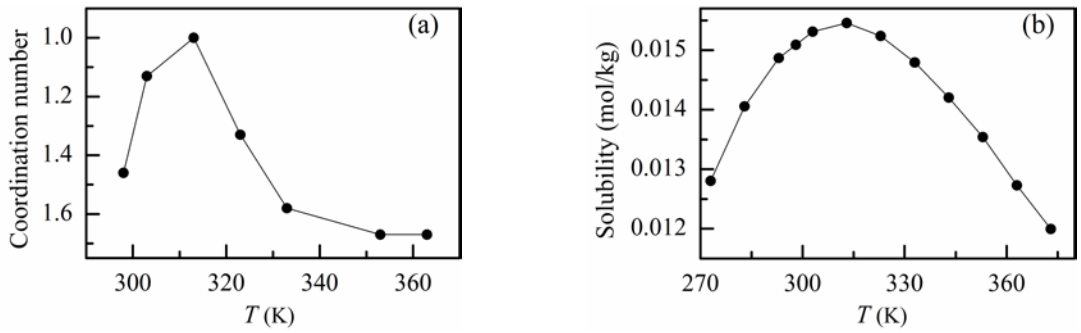

Fig. S10 (a) Temperature dependence of Ca-S coordination number in 0.031 mol/kg $CaSO_4$ aqueous solutions; (b) Solubility of calcium sulfate dihydrate in water as function of temperature (Data from Marshal et al.[6] and Knacke et al.[7]).

In order to further examine the relation between ion association and the $CaSO_4$ solubility, the temperature dependence of ion association in aqueous solution was examined based on the Ca-S coordination number in aqueous $CaSO_4$ solution (The coordination number of Ca-OS can only partially reveal the degree of ion association). Ion association is strengthened as temperature increases in $CaCl_2$ solution,[8] but the situation is different in $CaSO_4$ solution. The $CN_{Ca\text{-}S}$ firstly decreases with increasing temperature (< 313 K), in Fig. S10(a). At about 313 K, there appears to be a minimum for the value of $CN_{Ca\text{-}S}$. Beyond this temperature, there is an abrupt increase of the $CN_{Ca\text{-}S}$, owing to the enhancement of ion association. The bridging hydrogen bonding between water molecules in the hydration layer of Ca^{2+} and the oxygen atom of SO_4^{2-} will be flexible as temperature increases (> 313 K), and thereby the role of such hydrogen bonding on the stabilization

of $CaSO_4$ will be weakened. It is also interesting to notice that the temperature, at which the $CN_{Ca\text{-}S}$ reaches the minimum, roughly coincides with the temperature, at which the observed solubility of calcium sulfate dihydrate reaches a maximum (in Fig. S10(b)).[6, 7] Therefore, ion and counter-ion association degree in these classical MD simulations at various temperatures, meaningfully shows the experimental solubility trend of calcium sulfate dihydrate with temperature, from the microscopic point of view.

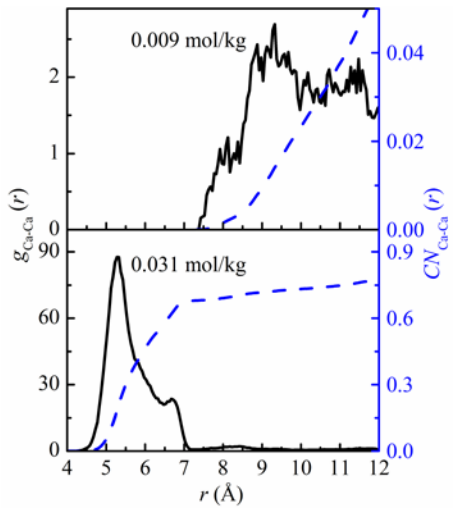

Fig. S11 The radial distribution function ($g(r)$) represented by the solid lines, and the coordination number (CN), represented by the dashed lines for Ca^{2+} and Ca^{2+} in 0.009 mol/kg and 0.031 mol/kg aqueous $CaSO_4$ solution, as obtained from the last 4 ns of the classical MD run. The relatively close Ca-Ca distance in 0.031 mol/kg aqueous $CaSO_4$ solution predicts that the strong ion association trend in supersaturated $CaSO_4$ aqueous solution.

References

1. J. Åqvist, *J. Phys. Chem.*, 1990, **94**, 8021-8024.
2. W. R. Cannon, B. M. Pettitt and J. A. McCammon, *J. Phys. Chem.*, 1994, **98**, 6225-6230.
3. H. J. C. Berendsen, J. R. Grigera and T. P. Straatsma, *J. Phys. Chem.*, 1987, **91**, 6269–6271.
4. G. Bai, H. B. Yi, H. J. Li, J. J. Xu, *Mol. Phys.* **2012,** *111*, 553–568.
5. W. L. Jorgensen, C. Jenson, *J. Comput. Chem.* **1998,** *19*, 1179–1186.
6. W. L. Marshal and R. Slusher, *J. Phys. Chem.*, 1966, **70**, 4015–4027.
7. O. Knacke and W. Gans, *Zeit. Phys. Chem., NF*, 1977, **104**, 41.
8. Q. Dai, J. J. Xu, H. J. Li and H. B. Yi, *Mol. Phys.*, 2015, **113**, 3545–3558.